

High density H₂ and He plasmas: can they be used to treat graphene?

H-A. Mehedi,¹ D. Ferrah,² J. Dubois,¹ C. Petit-Etienne,¹ H. Okuno,³ V. Bouchiat,⁴ O. Renault² and G. Cunge¹

¹ Laboratoire des Technologies de la Microélectronique, CNRS-UJF, 17 rue des Martyrs, 38054 Grenoble, France.

² CEA, LETI, MINATEC, 17 rue des Martyrs, 38054 Grenoble, France.

³ CEA, INAC/SP2M/LEMMA, 17 rue des Martyrs, 38054 Grenoble, France.

⁴ Institut Néel, CNRS-UJF-INP, BP 166, 38042 Grenoble cedex 9, France

Abstract

Since graphene and other 2D materials have no bulk, a major issue is their sensitivity to surface contaminations, and the development of cleaning processes is mandatory. High density plasmas are attractive to treat (clean, dope, pattern) 2D materials because they are a mature industrial technology adapted to large area wafer. However, in these plasmas the substrate is bombarded by a high flux of both thermal radicals and reactive ions with typical energy above 10 eV, which can easily damage atomic layer thin materials. We have investigated systematically the interaction of H₂ and He inductively coupled plasmas (ICP) with graphene in industrial reactors. We report a specific issue associated with the use of H₂ plasma: they etch the inner part of plasma reactor walls, thus releasing impurities in the plasma, most notably O atoms that etch graphene and Si atoms which stick on it. The presence of parasitic oxygen presumably explains the discrepancies found in the literature regarding the impact of reactive plasmas on graphene damages. To get rid of this issue we propose to use a fluorinated aluminum chamber. In this case, fluorine atoms which are shown to be harmless to graphene are the only impurity in the plasma. Under such conditions H₂ ICP plasma is shown to clean graphene without damages if the ion energy is kept below about 15 eV.

1. Introduction

The fabrication of electronic devices requires many technological steps including surface cleaning and preparation, doping and patterning. With the development of artificial structures based on 2D materials, these technologies must be revisited to accommodate stacks of atomically thin layers. In particular, reactive plasma processes which are key technologies in semiconductor manufacturing are not necessarily compatible with such fragile layers. For instance, H₂, Ar, O₂ and He plasmas have been used to clean polymeric residues from graphene [1-4], to pattern graphene [5-10] and to trim laterally graphene nanoribbons [11-13]. The key issue when dealing with plasma processes of graphene is plasma induced damages, which can be caused either by

chemical reactions with reactive radicals (chemisorptions, etching) or by energetic ions (sputtering) [1, 4-6, 16-22].

Four different types of plasma sources have been used to treat graphene: downstream plasmas in which the surface is exposed only to thermal radicals (O, H, etc...) [1, 4, 7, 21-23]; high density plasma sources in which the sample is bombarded by high fluxes of radicals and ions but with relatively low energy ions (10–150 eV) [2, 3, 12, 24-26]; capacitively coupled plasmas in which the sample is bombarded by a low flux of very energetic ions (typically > 100 eV) [10] and finally, low electron temperature (T_e) plasma or pulsed inductively coupled plasma (ICP) can be used to generate a small flux of low energy ions (1-10 eV range accessible) [27].

Although the results greatly depend on the plasma conditions and especially the plasma chemistry, the global trend is that low ion energy bombardment is mandatory to prevent the etching of the graphene layer. For instance, experiments performed with Ar ion beams to clean graphene [4, 28] have revealed that above 10 eV energy the graphene lattice is irreversibly damaged.

Indeed, several recent reports [7, 22, 23, 27] suggest that both Low T_e plasmas and downstream ICP generate much less damages to graphene than a typical ICP. However, several other studies [2, 24, 25] carried out in typical ICP regime (high ion flux) in Cl_2 or H_2 plasma have shown that ICP reactors are efficient to dope and clean graphene without causing irreversible damages to the graphene lattice. The case of H_2 plasma is particularly interesting because it has been studied extensively for a broad range of applications (cleaning and doping of graphene sheets [2, 3, 24, 25], to pattern graphene [7, 29, 30], to etch laterally nanoribbon [15, 31], to produce graphane [32] or to store hydrogen [33]). However, contrasting results have been reported by several groups [26, 34-36] under apparently similar experimental conditions, and severe damages have been reported even in downstream H_2 plasmas [1, 21].

Such discrepancies can be due to many reasons, the simplest one being that the flux and energy of the particles that bombard graphene strongly vary from one reactor to another. There is another important source of variability when dealing with atomically thin layers: the presence of impurities in the discharge that may damage graphene or contaminate its surface. Such impurities can originate from the etching of the reactor vessel and can interact dramatically with the material being treated. As a matter of fact, managing the reactor walls is a considerable issue in typical processes used for integrated circuit fabrication, and sophisticated coating/cleaning strategies (between each processed wafer) have been implemented in this field to ensure process reproducibility [37, 38].

In this work, we have analyzed the impact of the contaminants released from the inner part of plasma reactor walls and substrate holder when graphene is exposed to H_2 and He ICP plasmas. Using X-ray Photoelectron Spectroscopy (XPS) and Transmission Electron Microscopy (TEM), we show that halogens, metallic and O impurities originating from the etching of the reactor walls or wafer holder are present in these plasmas. As a result, if no attention is paid to the reactor vessel material, graphene is etched by O atoms and/or contaminated by metals and halogens. In this paper, we have investigated several reactor wall coatings and analyze their impact on graphene. This allows us to propose a specific reactor coating strategy to treat

graphene without damages since under these conditions F atoms, which are harmless to graphene, are the only impurity in the plasma.

2. Experimental

Plasma treatment is carried out in a high-density inductively coupled plasma (ICP) source (DPS AdvantEdge™) from Applied Materials designed to etch 300 mm diameter wafers and described elsewhere [43]. The inner part (lining) of the reactor is typically made of Al₂O₃ material which can be replaced with SiO₂ or Y₂O₃ liners. In all the experiments described below, the wafer temperature is kept at 65 °C by helium backside cooling (electrostatic chuck). However, the sample temperature can increase during long plasma experiments due the reduced thermal coupling between the sample and the wafer. The reactor is modified to be connected to an XPS system by a robotized vacuum transfer chamber allowing quasi in-situ analysis. The chamber is also equipped with plasma diagnostic techniques, including ion flux probe [44, 45] to measure the ion flux and retarding field electrostatic multigrid analyzers [46] to measure the ion velocity distribution function at the wafer surface. The ICP plasma can be operated in continuous wave (CW) mode or in pulsed mode [47], in which the RF power is turned ON and OFF periodically at high frequency. In pulsed mode at low duty cycle both the ion flux and ion energy are very low and the plasma conditions are basically comparable to those obtained in a downstream reactor since [46]. To improve the wafer-to-wafer reproducibility, the ICP reactor is cleaned using typical industrial cleaning process [48] with an SF₆-based plasma (SF₆/O₂ plasma) in between each experiment. Three different carrier wafers of 300 mm diameter are used to introduce and hold small graphene samples in the reactor: Aluminium (Al), Aluminium Oxide (Al₂O₃; 20 nm Al₂O₃ deposited on 500 μm thick Silicon wafer by plasma CVD) and Silicon (Si) wafers. The graphene samples are stuck with kapton™ tape on the carrier wafer.

Samples treated in this study are commercially produced monolayer graphene sheets from Graphenea S.A. We use three different types of graphene samples: as-grown CVD graphene on Cu foil, PMMA-assisted transferred CVD graphene on SiO₂ (300 nm thick)/Si and Si (with native SiO₂) substrates.

XPS measurements over an area of few mm² were carried out at a base pressure of 10⁻⁹ mbar with a customized Thermo Electron Theta 300 spectrometer using a monochromatic X-ray source Al-Kα (1486.6 eV). The emitted photoelectrons are collected using an electrostatic lens with 60° angular acceptance. The axis of the lens is 50° from the sample normal, enabling electron collection ranging from 20° to 80°. The overall energy resolution of the analysis is 0.4 eV. The Spectrometer is directly connected under vacuum to the plasma chamber through a robotized transfer chamber. This experimental configuration prevents surface contamination between the plasma process and the XPS analysis, thereby allowing a quasi-in-situ analysis condition of plasma-treated graphene surface. The XPS spectra were fitted using standard procedures, i.e. Shirley background subtraction and resolution into Doniach-Sunjic function for *sp*² graphene-related component and Voigt function for the other components.

Atomic resolution TEM imaging was performed using a low-voltage aberration corrected microscope (Titan Ultimate-FEI at 80 kV) in order to observe the sample before and after the

plasma treatments. Monolayer graphene was transferred on Si_3N_4 quantifoil TEM grids with 1 μm diameter holes and then treated by the H_2 plasma. Transfer was done using standard procedures, i.e. etching of Cu foil using aqueous solution or graphene delamination from Cu by electrochemical process, and transfer of resulting free standing PMMA on graphene film on new support, in which PMMA was removed in acetone, leaving behind persistent PMMA residues. Due an adhesion issue of graphene on the silicon nitride TEM grids and to the inherent fragility of suspended graphene, it was necessary to treat the graphene transferred on the grids in a pulse plasma at same pressure and power as before (the ion energy is reduced to 1-5eV in pulsed mode). XPS measured directly on TEM grid indicates that the final result is the same in pulsed and CW modes.

3. Results and Discussion

3.1 The issue of the chamber walls: the necessity of coatings

In typical high-density plasma (HDP) sources, the wafer is bombarded by a high flux of reactive radicals and by energetic ions, which may result in the etching of graphene or on the grafting of radicals at the graphene surface. However, while radicals can easily chemisorb on dangling bonds (vacancies, defects, edges of graphene nanoribbons), they often cannot stick on pristine graphene which is protected by an energy barrier formed by the π -electron cloud of graphene. For instance, an H atom with energy less than 0.4-0.6 eV cannot chemisorb on a pristine graphene surface [49]. Since radicals in plasmas have typically an energy less than 0.1 eV, they remain inert toward graphene. Therefore, in many cases only the positive ions whose energy is typically above 10 eV in HDP sources can chemisorb on graphene. One notable exception is atomic O which reacts spontaneously (barrier less) with the graphene to form CO and CO_2 etch products [50, 51]. The presence of parasitic oxygen in the plasma should, therefore, be considered as a serious issue, and must be prevented. However, we find that O-free conditions are highly difficult to obtain both in He and H_2 plasmas when they are operated in typical plasma reactors. To illustrate the issue, we first operated the plasma in a clean plasma chamber entirely made of Al_2O_3 . To do so, we run the plasma of interest (He/ H_2) for a few minutes before introducing the sample to the sputtered impurities from the Al_2O_3 chamber walls. Indeed, our industrial ICP reactor is periodically cleaned by SF_6 plasma to ensure process reproducibility [48, 52]. Note that industrial ICP reactors are typically used in Front End processes, i.e. to etch semiconductor and metals in halogen based plasmas. Since these processes deposit metallic impurities on the reactor walls, the industry has introduced waferless chamber cleaning processes to ensure wafer to wafer reproducibility. Those clean are F-based, typically SF_6/O_2 or NF_3/O_2 . This treatment fluorinates the Al_2O_3 chamber walls, transforming their surface in AlF_3 and leading to the absorption of F inside the ceramic pores. By operating the plasma for a few minutes, most of the F originating from the SF_6 cleaning plasma is sputtered from the chamber walls which are then turned to a F-poor AlOF_x material. The reactor with these conditions is referred to a “clean reactor” even though significant amount of F atoms are released from these walls both in He and H_2 plasmas, as discussed below.

He plasma treatment. Figure 1 shows the XPS spectra of CVD graphene on Cu before and after exposure to a low power (50 Ws) He ICP plasma operated in the clean reactor.

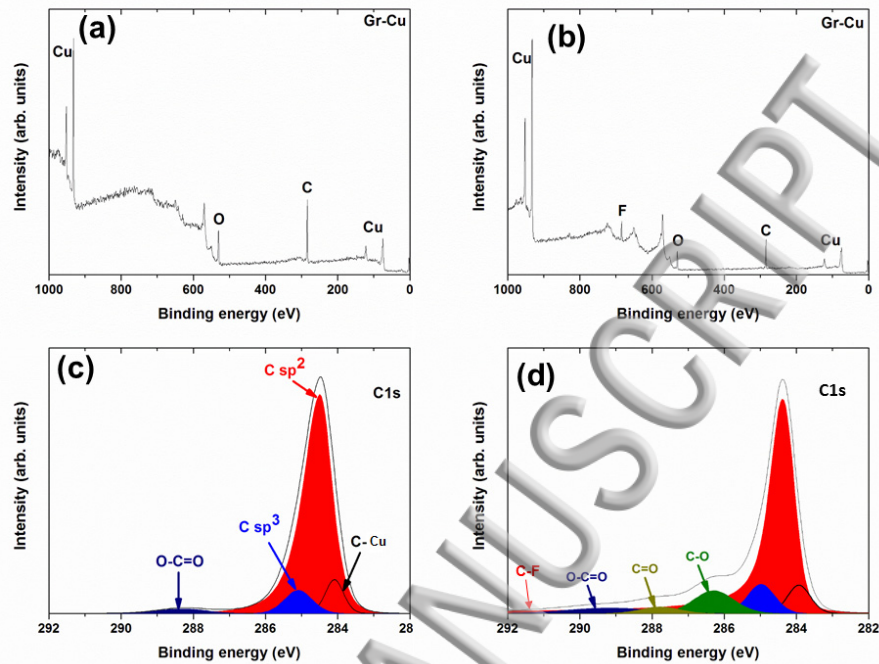


Figure 1. (a-b) Survey XPS spectra measured on CVD graphene/Cu: (a) reference before He plasma treatment and (b) after He plasma treatment in a clean reactor with chamber walls made of Al₂O₃. (c-d) Corresponding C1s XPS spectra: (c) before and (d) after He plasma treatment revealing the presence of parasitic oxygen and fluorine atoms in the plasma. Prior to He plasma treatment, the ICP reactor is first cleaned with SF₆ plasma [48, 52]. Then, He plasma is run first without the graphene sample and then with the sample. The small graphene sample is fixed on a Si wafer of 300 mm diameter. The He plasma treatment conditions are as follows: 50 W ICP power, 300 mT chamber pressure, 30 sec treatment time and 200 sccm He flow.

The presence of C-O and C=O bonds after the plasma treatment (as shown in the C1s spectrum in figure 1(d)) reveals the presence of parasitic oxygen atoms in the plasma. They originate from the chamber walls and/or the 300 mm Si (with a thin film of native SiO₂) carrier wafer under these conditions. He is a chemically inert gas, so it is either the physical sputtering by the He⁺ ion or the interaction of energetic photons or metastable He atoms, which sputters O from the Al₂O₃ walls and/or from the carrier wafer. We also observe the presence of parasitic F atoms bonded to graphene (figures 1(b,d)). They originate from the plasma interaction with the walls. Since F atoms cannot chemisorb on pristine graphene, their presence is indicating the formation of defects (vacancies, holes...) during the plasma, on which F can chemisorb due to the presence of dangling bonds [53, 54].

H₂ plasma treatment. In H₂ plasmas the situation is even more critical: in addition to the defects created by O atom etching and decorated by F atoms we also find significant amounts of silicon

adsorbed at the graphene surface, as evidenced by XPS (about 25% of Si is detected at the surface, figure not shown here) and by the HRTEM image (figure 2) which shows that Si atoms are covering the surface (graphene and PMMA residues) progressively.

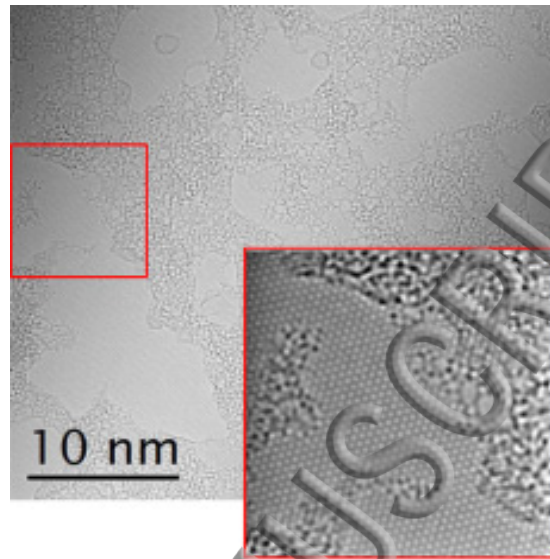


Figure 2. HRTEM image of CVD monolayer graphene transferred on Si_3N_4 TEM grid after H_2 plasma treatment. The red square and the associated inset indicate a region where several layer-thick PMMA is observed. These regions are systematically associated with the presence of heavier silicon impurity atoms (that appears darker) especially on the edges of the flakes of residues. Prior to H_2 plasma treatment, the ICP reactor is first cleaned with SF_6 plasma [48, 52]. Then, H_2 plasma is run first without the graphene sample and then with the sample. The small graphene sample is fixed on a Si wafer of 300 mm diameter. The H_2 plasma treatment conditions are as follows: 800 W ICP power, 200 mT chamber pressure, 30 sec treatment time and 200 sccm H_2 flow.

In an Al_2O_3 chamber, this parasitic silicon can only originate from the etching of the 300 mm diameter Si (or SiO_2) wafer, which serves as a substrate holder for the small graphene samples. The Si atoms etched from this substrate in the form of SiH_x is easily dissociated and ionized by electron impact reaction in the plasma [55] and redeposited on the graphene sample.

To further highlight the chamber wall issue, we performed similar plasma treatment in the Al_2O_3 chamber, but using a 300 mm diameter Al_2O_3 wafer; this wafer, which can be transported under vacuum to the XPS analyzer, is used to simulate the chamber walls (same material) and to analyze the impact of He and H_2 treatment on their aging. Figures 3 (a-b) show the $\text{Al}2p$ XPS spectra before and after 20 minutes of exposure to a high density H_2 plasma. After the plasma, new contributions are observed in the Al peak and attributed to metallic aluminum i.e. Al-Al bonds. This indicates that the H_2 plasma reduces Al-O bonds by forming OH or H_2O volatile products which are desorbed in the plasma, thus acting as a source of O.

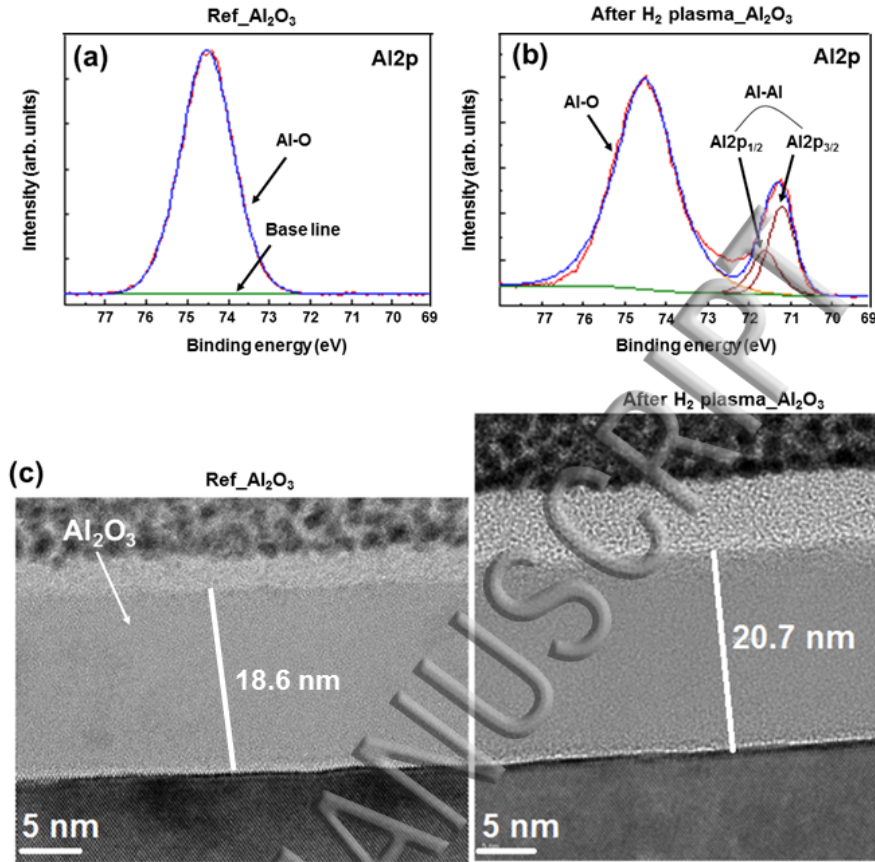


Figure 3. (a-b) XPS Al₂p spectra measured on the 300 mm diameter Al₂O₃ wafer (a) before and (b) after H₂ plasma treatment in a clean ICP reactor with Al₂O₃ chamber wall. (c) Cross-sectional HRTEM image of the same sample before and after the plasma treatment. Prior to H₂ plasma treatment, the ICP reactor is first cleaned with SF₆ plasma [48, 52]. Then, H₂ plasma is run first without the sample and then with the sample. The H₂ plasma treatment conditions are as follows: 800 W ICP power, 200 mT chamber pressure, 20 min treatment time and 200 sccm H₂ flow.

There is no etching of the Al₂O₃ layer but its top surface is reduced to become metallic, and the depth of the modified material increases with time. As shown in the TEM images in figure 3 (c), the Al₂O₃ is modified on a depth of about 4 nm after 20 minutes of plasma, and the total thickness of the sample is increased by 2 nm. This swelling of the layer strongly suggests the incorporation of H in the layer and perhaps the formation of cavities and bubbles. Furthermore, we have also detected significant amounts of F atoms on the sample by XPS (Table S1 in the supporting information (SI)). This F is released from the true reactor walls during the H₂ plasma and sticks to the Al₂O₃ sample. Interestingly, F is not covalently bonded to Al but seems to be physisorbed in the (rough) sample either in the form of F or more probably HF. On a longer term, the presence of such corrosive species could be another source of reactor wall degradation.

Similar H₂ plasma experiments performed in the ICP reactors with Y₂O₃ (the material of most modern chambers) and SiO₂ walls lead to the same observation and conclusions (data not shown

ing): in a high density H_2 plasma the metal-oxide parts of the reactor are reduced, thereby releasing O atoms in the plasma as well as Si atoms in the case of the SiO_2 chamber wall.

Therefore, He and H_2 plasmas operated in a “clean” plasma chamber damage the materials constituting the plasma chamber, releasing O atoms, halogens and metallic impurities in the plasmas. This is a considerable issue since these atoms will, in turn, damage the graphene irreversibly. From this observation one can conclude that a specific chamber (as well as the substrate holder) conditioning strategy must be implemented to treat graphene under controlled conditions. We will discuss the specific issues with the substrate holder in the section 3.

3.2 The influence of various chamber wall coatings

Coating the chamber walls by using an appropriate plasma before processing a wafer is a typical strategy used in the microelectronic industry to ensure wafer to wafer reproducibility during Si and metal etching processes. Typical coatings include SiO_x (deposited by $SiCl_4/O_2$ plasma), fluorination of Al_2O_3 or Y_2O_3 chamber walls with a SF_6 or NF_3 based plasma and carbon deposition from CH_x or CF_x plasmas. By analogy with the issue of SiO_2 wafer observed previously, the plasma deposited SiO_x coating is expected to release O and Si atoms in the plasma, and is not ideal for plasma treatment of graphene and other 2D materials which are sensitive to oxidation. Therefore, we have investigated the impact of fluorinated and carbon-coated chamber walls on the H_2 and He plasma treatment of graphene.

Carbon coating. Figure 4 shows XPS spectra of a CVD graphene/ SiO_2 /Si before and after H_2 plasma treatment in the carbon coated ICP chamber (C coating deposited by CH_4 plasma: 500 W ICP power, 5 mT chamber pressure, 100 sccm CH_4 , 60 sec).. The H_2 plasma treatment results in an increase of the C1s carbon peak intensity (Figure 4(b)), which demonstrates that there is deposition of carbon like materials on the graphene sample under these conditions. We underline that this deposit is extremely thin, probably a monolayer. To confirm this carbon contamination, we then analyze the C1s core level spectra before and after the plasma treatment (Figures 4(c-d)).

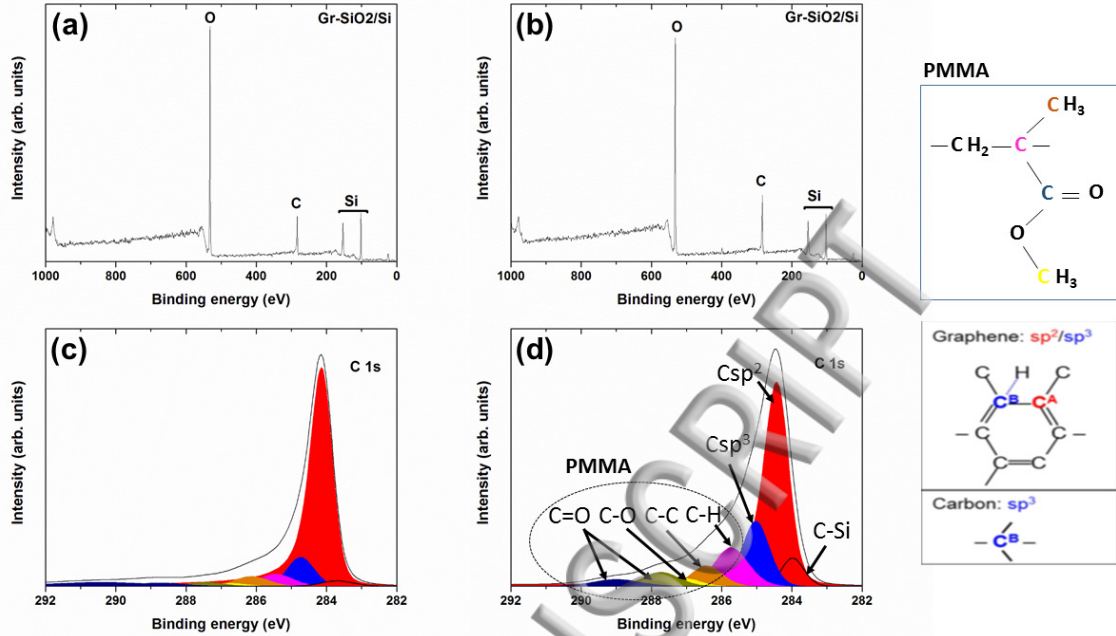


Figure 4. (a-b) Survey XPS spectra measured on graphene/SiO₂/Si: (a) reference before plasma and (b) after 30 sec H₂ plasma treatment. (c-d) corresponding C1s XPS spectra: (c) before and (d) after the plasma treatment. The increase in the carbon peak intensity in (b) indicates the contamination of the graphene surface with carbon released from the reactor wall during the plasma treatment, as is also confirmed by the increase in the carbon containing components in graphene as well as in PMMA (d). The inset on the upper right hand side is a schematic representation of the various carbon components present in PMMA and graphene. Prior to H₂ plasma treatment, the 300 mm diameter Al₂O₃ carrier wafer was treated with SF₆/O₂ plasmas, and the ICP reactor was treated with CH₄ plasmas. Therefore, the surface of the Al₂O₃ carrier wafer is fluorinated while the chamber walls are coated by a thick layer of carbon. Then, the H₂ plasma treatment was carried out with the following conditions: 800 W ICP power, 200 mT chamber pressure, 30 sec and 200 sccm H₂.

The measured C1s curve of the graphene/SiO₂/Si before H₂ plasma treatment can be fitted with the contribution of six components. The main asymmetric peak observed at 284.4 eV binding energy is characteristic of C=C bonds (*sp*² component) in graphitic carbon [56]. The second *sp*³ component at 285.0 eV is mainly assigned to amorphous carbon (as C–C, C–H bonds) commonly observed in CVD-grown graphene [57]. A third component located at 284.0 eV is attributed to graphene-Si (C–Si) bonding at the interface and/or to presence of single vacancies [58]. The remaining four smaller C1s components at 285.7 eV, at 286.4 eV, at 287.1 eV and at 288.9 eV are assigned, respectively, to different chemical environments of carbon atoms in PMMA residues, for example, C–H, C–C, H–C–O and O–C=O bonds [59].

The C1s spectrum of the same sample after 30 sec H₂ plasma exposure (Figure 4 (d)) shows an increase of all the contribution of the C1s peak including the *sp*² component, suggesting the presence of additional carbon residues. The increase in C-Si contribution is attributed to plasma induced reactions between SiO_x contaminants (initially present on graphene) and carbon atoms originating from graphene or from atmospheric contaminants: it has been shown [2] that SiO_x

mp particles are decomposed and spread on the surface under H₂ plasma treatment. Since the small graphene sample is placed on a fluorine coated Al₂O₃ carrier wafer during plasma exposure, the redeposited carbon clearly originates from the erosion of the carbon coating on the chamber walls which release C_x and/or C_xH_y radicals in the plasma. It is interesting to underline that the H₂ plasma is etching the amorphous carbon deposited on the chamber walls at a high rate. Therefore, it is surprising to observe carbon deposition on graphene in the same plasma at the same time. By analogy with 2D PMMA^G residues [60, 61] we believe that the redeposited carbon contains aromatic cycle or linear chains which stick onto graphene by pi-stacking: this explains why some of the redeposited carbon is not etched away by H atoms.

High density He plasma performed in the same carbon-coated chamber leads to similar observations (Figure S1 in the SI) even if He is chemically inert: there is some carbon eroded from the reactor walls and redeposited on the graphene. Carbon etching from the chamber walls could be due to He⁺ ion bombardment to the walls (physical etching) or from photon/metastable assisted etching of carbon. We thus conclude that the carbon coating is not ideal for treating graphene in He and H₂ plasmas.

Fluorine coating. In the case of the AlF₃ coatings (formed by SF₆/O₂ plasma as described in the SI) on the chamber walls and the Al₂O₃ carrier wafer, we first observe a decrease of the carbon peak intensity (by about 50%) in the XPS survey spectra of graphene/SiO₂/Si (Figure 5(b)) after 90 sec exposure to H₂ plasma, which could be due to the removal of PMMA residues.

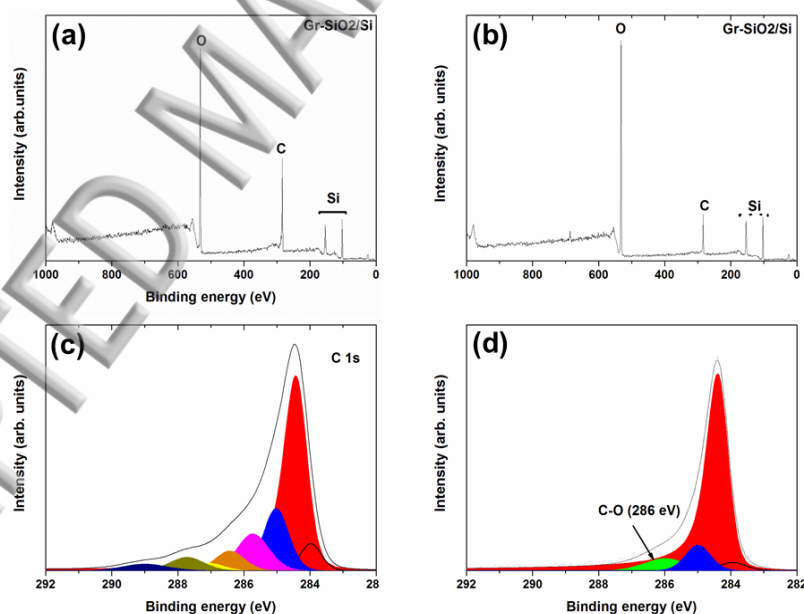


Figure 5. (a-b) survey XPS spectra measured on graphene/SiO₂/Si; (a) reference before plasma and (b) after H₂ plasma treatment. (c-d) corresponding C1s XPS spectra; (c) before and (d) after H₂ plasma treatment indicating removal of various carbon components in PMMA as well as removal of carbon residues in graphene as confirmed by the decrease in Csp³ peak intensity (blue curve in (d)). The appearance of the C-O peak, as indicated by arrow in (d), suggests graphene contamination with oxygen. Prior to H₂ plasma treatment, both the carrier wafer and the ICP reactor were treated with SF₆/O₂ plasmas.

Under these conditions, both the chamber walls and the wafer holder are fluorinated alumina. Then, the plasma treatment was carried out in 2 steps: step-1) 800 W ICP power, 200 mT chamber pressure, 30 sec, 200 sccm H₂, step-2) 800 W ICP power, 80 mT, 60 sec, 200 sccm H₂.

The comparison of the C1s spectra before and after plasma exposure (Figures 4(c-d)) indicates that there is no more PMMA residues remaining on graphene. The decrease in C *sp*³ contribution indicates removal of pre-existing amorphous carbon residues from graphene. The weak peak at ~286 eV binding energy is due to a small contamination by hydroxyl groups, such as C-O (i.e. -OH react with graphene to produce C-O groups) [58]. However, this C-O contribution is not attributed to PMMA residues, which are fully eliminated (indeed, a more prolonged plasma exposure results in an increase of this peak, figure not shown here). The most likely source of this oxygen is thus the reduction of the 300 nm SiO₂ layer underneath graphene. Indeed, under our conditions H_x⁺ ions can pass through the graphene layer without damaging it (as evidenced by the C1s peak in figure 5(d) and Raman spectra shown in Figure 10) and then becomes intercalated [62]. The H atoms trapped between the SiO₂ and graphene layer can partially reduce SiO₂ resulting in free OH radicals which bond to graphene at the interface [63]. This assumption is supported by the Si2p XPS spectra (Figure 6) of the same graphene/SiO₂/Si sample: after 30 sec H₂ plasma, a new contribution (SiO_{x1}) is observed at lower binding energy (~101 eV) compared to the principal SiO₂ peak, which corresponds to the contribution of sub-oxides i.e. SiO_x with x < 2 (Figure 6(b)).

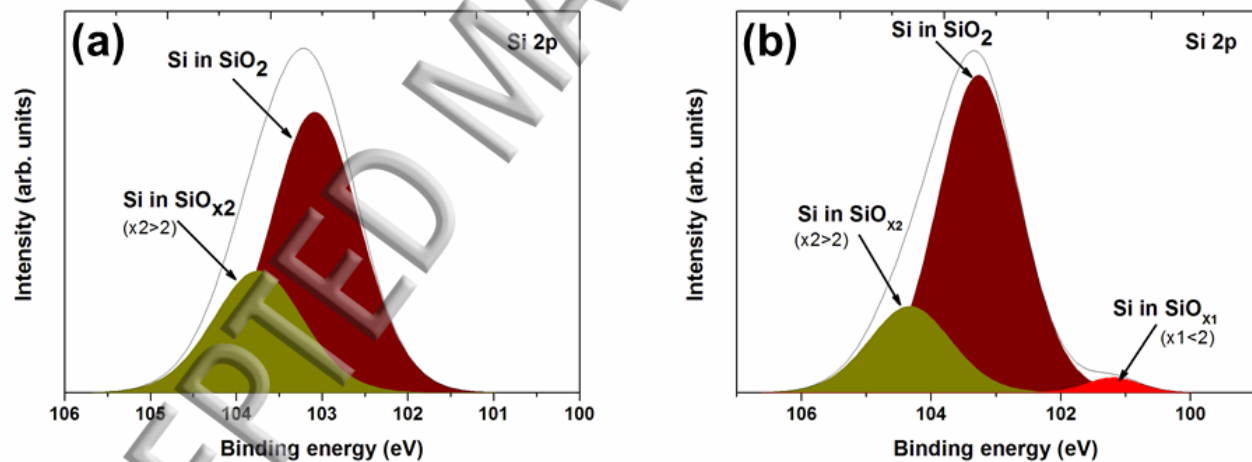


Figure 6. Si2p XPS spectra of graphene/SiO₂/Si; (a) reference before H₂ plasma treatment and (b) after H₂ plasma treatment in the fluorine-coated ICP reactor with fluorine coated 300 mm carrier wafer (20 nm Al₂O₃ on 500 μm Si). The appearance of the SiO_{x1} peak in the lower binding energy (d) demonstrates a partial reduction of the 300 nm SiO₂ layer underneath graphene during H₂ plasma exposure. The plasma treatment was carried out in 2 steps: step-1) 800 W ICP power, 200 mT chamber pressure, 30 sec, 200 sccm H₂, step-2) 800 W ICP power, 80 mT, 60 sec, 200 sccm H₂.

The underneath SiO₂ layer is thus reduced by H through the graphene layer. As discussed in the section 4, this may cause some issues (such as graphene lift-off) if an excessive amount of gas becomes intercalated underneath a graphene layer [62].

On the other hand, only traces of F atoms are observed in the survey spectrum (Figure 5(b)), attesting that graphene is not damaged. Indeed, there is no CF_x contribution in the C1s spectrum (Figure 5(d)) suggesting that F is not covalently bonded to carbon atoms in graphene but rather physisorbed, either in the form of F or more probably HF.

Interestingly, the O atoms released from the SiO₂ layer and later bound to graphene do not lead to graphene etching while O atoms from the plasma are found to etch graphene spontaneously as discussed previously. One possible explanation is that O atom chemisorption, which requires a *sp*² to *sp*³ re-hybridization of the C atom involved, bends the graphene surface (thus makes it fragile) more when chemisorption is on the top (facing the plasma) than on the bottom (intercalated) due to the finite distance between the substrate and the graphene sheet [64].

We also underline that similar results are obtained with graphene transferred on Si substrate (Figure S2 in the SI) leading to the conclusion: H₂ plasma in the AlF₃ conditioned ICP reactor with fluorine coated Al₂O₃ carrier wafer is an effective strategy to clean PMMA residues from transferred graphene irrespective to the underlying substrates. Note that a thin native SiO₂ layer is also detected between graphene and Si substrate in the case of graphene/Si sample.

In contrast, the He plasma treatment of graphene with similar fluorine conditioning of the chamber walls and the carrier wafer leads to graphene damages. The extent of the damage, however, varies depending on the ICP power, chamber pressure and treatment time. For instance, at high ICP power (> 200 W) we observe a complete etching of graphene within 30 sec of the treatment (Figure 7(a)). For the same treatment time at lower powers (150 and 100 W) there is a partial etching of graphene with significant damage in graphene lattice as evidenced particularly by the increase of C *sp*³, C-Si contributions and by F atoms covalently bonded to graphene in the form of CHF and CF₂ (Figures 7(e-f)).

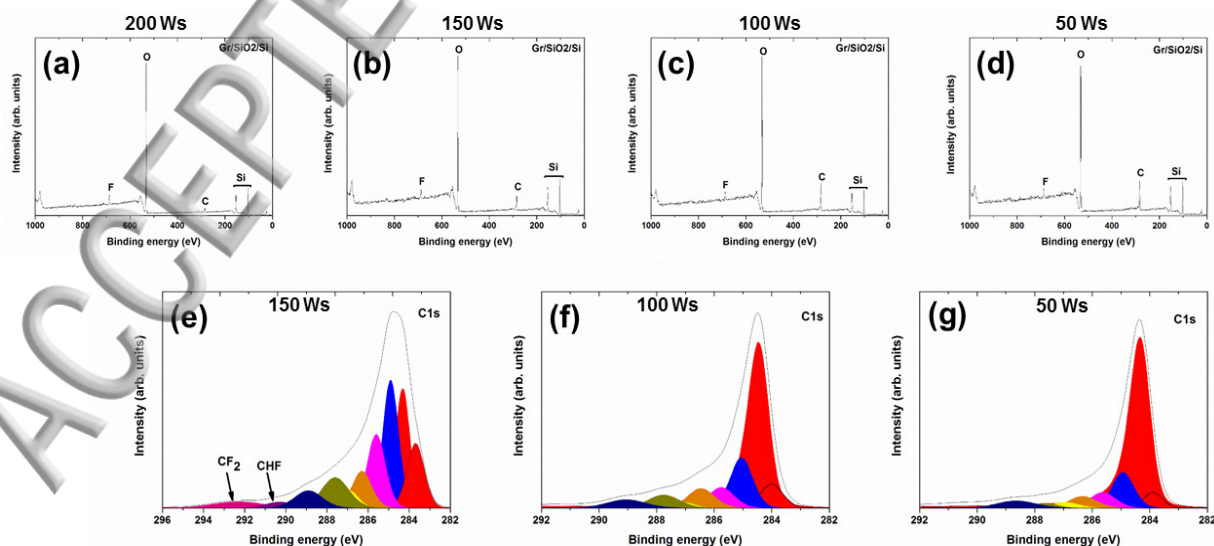


Figure 7. (a-d) Survey XPS and (e-g) corresponding C1s spectra measured on He plasma treated graphene/Cu at different ICP powers with fixed chamber pressure (300 mT) treatment time (30 sec) and He flow rate (200 sccm). The plasma treatment is carried out in the fluorine-coated ICP reactor with graphene/Cu fixed on the fluorine coated 300 mm Al₂O₃ carrier wafer.

Finally, at low power (50 W) there is no evidence of important graphene damage (except a very little amount of F atoms physisorbed to graphene (Figure 7(d)) and under these conditions the He plasma has removed some of the PMMA residues. However, even at such low power, graphene is slowly etched away with continued exposure to 50 W He plasma instead of being cleaned, as shown in figure S3 in the SI. We also observe that graphene is instantly etched when the chamber pressure is reduced below 40 mT irrespective to the ICP power and treatment time, as shown in figure S4 in the SI. These observations suggest that graphene damages are caused by the ion bombardment in He plasmas, which wasn't the case in H₂. There are two possible reasons for such discrepancies. First, it is known [65] that the predominant ion in H₂ plasma is H₃⁺, which splits into 3 H atoms at the impact with the surface: the initial energy of H₃⁺ is shared between these fragments, which minimizes the risk of surface damage by sputtering. Second, the ionization energy threshold of the parasitic species present in the plasma can be lower than that of the gas, leading to the formation of chemically reactive heavy ions [66]. The ionization energy of some common impurities are as follows [67]: Al (6 eV), Si (8.1 eV), C (11.3 eV), O (13.6 eV), F (17.4 eV). This is to be compared to the ionization energy threshold of He (24.6 eV), H₂ (15.4 eV) and O (13.6 eV) [67]. Therefore, one major difference between H₂ and He plasma is that due to the high ionization energy of He *all* the parasitic species released from the reactor wall will be ionized and bombard graphene with an energy higher than 15 eV: this energy is enough to overcome energy barriers and chemisorb on graphene, but also to sputter C atoms from the lattice. This is why damages are systematically observed in He. By contrast, in H₂ plasma Si, Al, C can be ionized, but neither F nor O, which explains why there is no irreversible damages to graphene in H₂ plasma operated in an AlF₃ coated chamber where F is the only impurity. In summary, the fluorine coating is not resistant to He plasma leading to F contamination, and the He plasma, being chemically inert, is not effective to remove PMMA residues from graphene, in contrast to H₂ plasmas.

3.3 The need of specific carrier wafer

A 300 mm wafer must be used to introduce and hold the small graphene small in our ICP reactor during plasma exposure. We analyzed the impact of the nature of the 300 mm wafer on graphene damage in the case of a Silicon wafer, a fluorinated Al wafer and a fluorinated Al₂O₃ wafer. In the three cases, the ICP chamber is preconditioned with SF₆/O₂ plasma leading to fluorine coating to chamber walls. Graphene sample is then placed around the center of the carrier wafer.

In the case of the Si carrier wafer we observe a severe Si contamination of the graphene after the H₂ plasma treatment (Figure 8(a)).

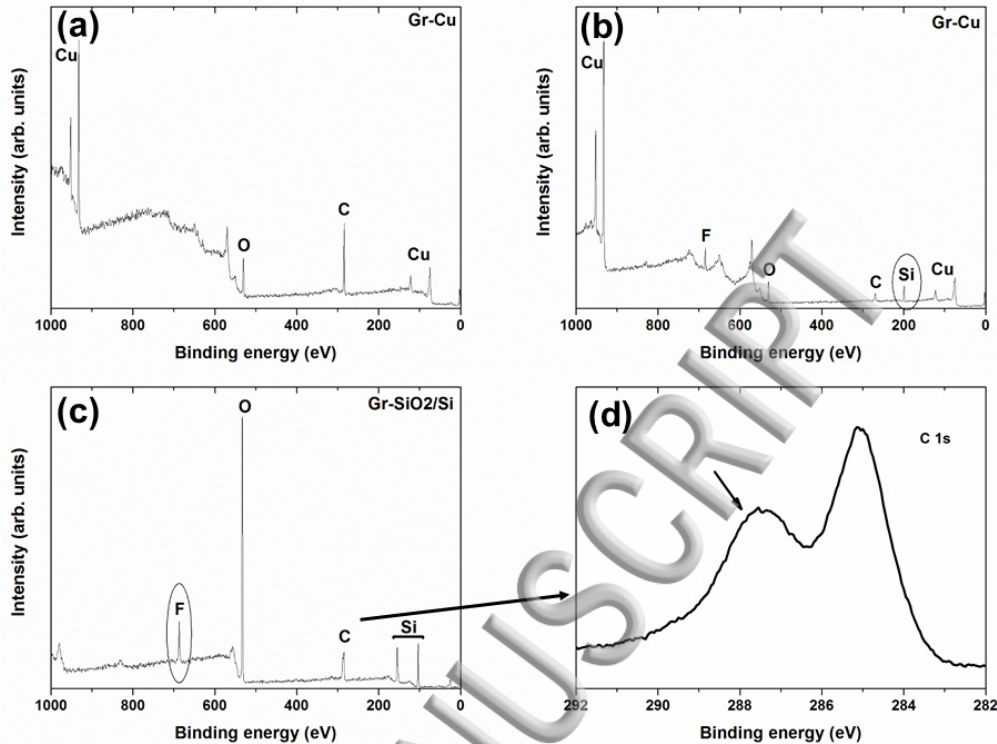


Figure 8. Survey XPS spectra measured on H_2 plasma treated graphene/Cu and graphene/ SiO_2 /Si with different carrier wafers. (a) reference graphene/Cu before H_2 plasma treatment and (b) after H_2 plasma treatment in the fluorine coated ICP reactor with 300 mm Si carrier wafer indicating graphene etching as well as contamination with Si. (c) graphene/ SiO_2 /Si after H_2 plasma treatment in the fluorine coated ICP reactor with fluorine coated 300 mm aluminum (Al) carrier wafer indicating graphene contamination with fluorine and (d) corresponding C1s spectrum shows appearance of C-F component confirming fluorine contamination. The plasma treatment was carried out with the following conditions: 800 W ICP power, 200 mT chamber pressure, 30 sec and 200 sccm H_2 .

To evidence this contamination, we have used graphene/Cu instead of graphene/ SiO_2 . Furthermore, the graphene layer has been partially etched as evidenced by a strong decrease of the C peak intensity as well as a significant F contamination of the sample. The case of the F-Al wafer (Figures 8 (c)-(d)) is quite similar: graphene is etched and some Al contamination of the surface is observed. The best result is obtained for F- Al_2O_3 (20 nm PECVD deposited Al_2O_3 on Si) carrier wafer resulting in effective cleaning of PMMA residues from graphene as discussed before (Figures 5 and S2 in the SI).

In the case of the Si wafer, the F atoms released from the AlF_3 chamber walls during the H_2 plasma exposure assist the etching of the Si wafer, and the SiF_x etch products are then dissociated and ionized before deposited to the graphene sample. Therefore, both Si and Al wafers are efficiently etched by H atoms (and F in the case of Si), while the fluorinated Al_2O_3 ceramic is more resistant. In fact, the material of construction of the plasma reactor is typically Al_2O_3 or Y_2O_3 due to the stability of these ceramics against the chemical attack by halogen atoms. The F- Al_2O_3 is highly resistant to H_2 plasma and this substrate releases only F atoms in the plasma

(exactly as the reactor walls do), which are harmless to graphene. By contrast, Si and Al are etched by F and H, releasing Si/Al and O atoms (from the thin and fragile native oxide layer at the wafer surface) in the plasma. The Si/Al are easily ionized, and since the Si^+ and Al^+ ions are heavy, they will sputter graphene and/or stick on it. Furthermore, the native SiO_2 oxide on the Si wafer releases O atoms at the beginning of the plasma leading to graphene etching, and the released F atoms are then decorated the generated defects. The fluorinated Al_2O_3 is thus the only solution we found to treat graphene.

3.4 The need of specific plasma conditions

Once one knows how to deal with the reactor wall and the wafer holder, there is still a need to optimize carefully the H_2 plasma cleaning process.

PMMA residues have been shown to be two types, referred to as PMMA^A and PMMA^G and follow different etching mechanisms due to their different chemical compositions [68]. For instance, PMMA^A are few nanometers thick, round-shaped amorphous residues and are easily etched by H atoms. PMMA^G residues, which have a 2D structure and contain aromatic cycles (mixture of sp^2 and sp^3 carbons) strongly adhere to graphene by pi-stacking [60, 61]. Since our H_2 plasma cleaning process etches selectively sp^3 hybridized carbon over sp^2 , PMMA^G residues are etched by H atoms but from their edges [7, 13, 69], a process which is long. Furthermore, there is another issue associated with cleaning, which limits the time available to clean graphene: the graphene lift-off effect. As shown in figure 5, H atoms get intercalated between graphene and SiO_2 and partially reduce SiO_2 layer. The trapped H atoms at the interface can also recombine to form H_2 gas eventually leading to a liftoff of the graphene layer when the trapped gas pressure (H_2 , OH...) overcomes the binding forces between graphene and the substrate [70, 71]. This phenomenon will be discussed in details in the upcoming paper but generate the need of a two step cleaning process in which a high pressure-short exposure (200 mT, 30 sec) step is followed by a lower pressure-longer exposure (80 mT, 60 sec), each step using 800 W ICP power with 200 sccm H_2 flow. The motivation for this procedure is that the cleaning process must thus be quick enough to remove all PMMA residues before the lift-off occurs. This is the goal of the two step process: in the high pressure step, there is a high density of H atoms to etch PMMA but the ion energy and flux are low. This low energy minimizes ion implantation through graphene (no risk of lift-off) but fails to completely remove the resistant PMMA^G residues (Figure 9(a)).

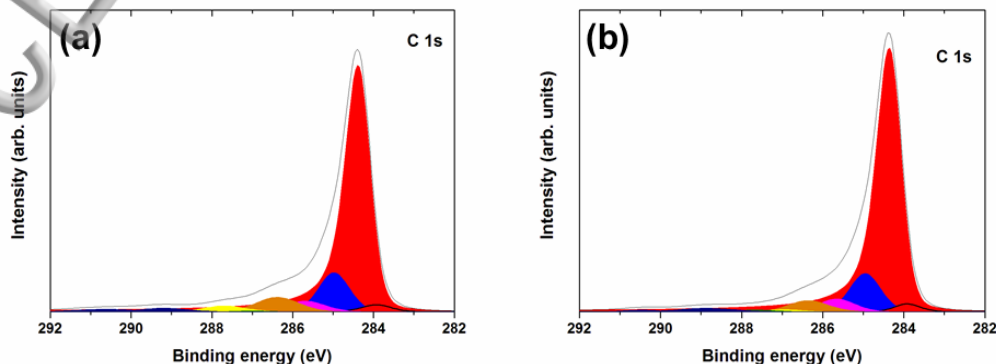


Figure 9. C1s XPS spectra measured on graphene/SiO₂/Si after treated with (a) H₂ plasma conditions of the step-1: 800 W ICP power, 200 mT chamber pressure, 30 sec, 200 sccm H₂ and (b) H₂ plasma conditions of the step-2: 800 W ICP power, 80 mT, 60 sec, 200 sccm H₂ indicating the presence of PMMA residues on the graphene surface after H₂ plasma treatment.

By contrast, the low pressure step is more efficient to clean residues but cannot be used alone to fully clean graphene because the lift-off takes place before graphene is fully cleaned: in figure 9(b) the C1s peak still show the presence of residues after 60 sec. If the treatment time is increased to 65 sec, there is no more carbon on the sample due to lift-off (Figure S3(c) in the SI). We therefore start at high pressure to remove as much PMMA as possible with minimal ion implantation, and the cleaning is then finished at low pressure.

3.5 Structural characteristics of the H₂ plasma cleaned graphene: Raman measurement

In Figure 10, we compare the Raman spectra of graphene/SiO₂/Si before and after plasma treatment as well as after annealing, recorded using 488 nm laser excitation.

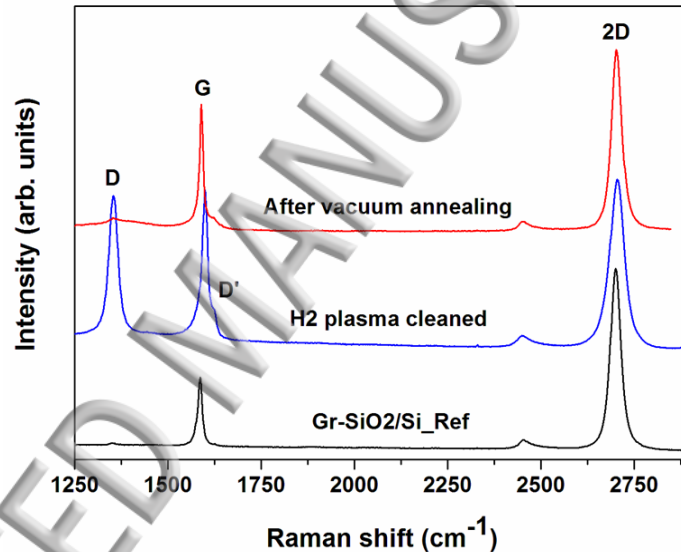


Figure 10. Raman spectra of graphene/SiO₂/Si (a) reference before H₂ plasma treatment, (b) after H₂ plasma treatment and (c) after vacuum annealing at 450 °C for 60 min. Laser wavelength was 488 nm. Prior to H₂ plasma, both the ICP reactor walls and the carrier wafer surface (20 nm Al₂O₃ on Si) were fluorine coated. The plasma treatment was carried out in 2 steps: step-1) 800 W ICP power, 200 mT chamber pressure, 60 sec, 200 sccm H₂, step-2) 800 W ICP power, 80 mT, 30 sec, 200 sccm H₂.

Before plasma, graphene surface is covered by a thin layer of PMMA residue, but no discernible Raman signals of PMMA (typically at 1450 and 1530 cm⁻¹) are seen when graphene is lying on a SiO₂/Si substrate. However, a clear background signal spanning from 1200 to 1500 cm⁻¹ appears for transferred graphene on Si substrate (Figure S5 (a) in the SI). The Raman spectrum of the reference graphene/SiO₂/Si shows distinct G and 2D peaks associated with long range ordered

graphitic sp^2 carbon (black curve in Figure 10) [72, 73]. The intensity ratio of the 2D to G peaks is, $I_{2D}/I_G = 2.78$, and the 2D peak (at 2700 cm^{-1}) can be well fitted with one Lorentzian peak with a width of 30.5 cm^{-1} . These factors indicate the presence of monolayer graphene [73, 74], and this monolayer signal is consistent over the entire 2 inch graphene sample. The fact that the D peak is very weak and the D' (which occurs via an intra-valley double-resonance process in the presence of defects) is absent, indicates a graphene layer of high crystallinity and low defect density [75]. In contrast, after H_2 plasma treatment (i.e. two steps treatment that effectively removes PMMA residues), a distinct D band together with weak D' are observed (blue curve in figure 10) suggesting generation of defects during plasma exposure. Both G and 2D are slightly broadened and upshifted indicating doping of graphene [76, 77]. The intensity ratio 2D to G peaks is now $I_{2D}/I_G = 1.01$. Encasement of defects could be responsible for the intensity reduction [75]. However, as shown in figure 10 (red curve), high vacuum annealing (under 10^{-9} mbar at 450°C for 60 min) of the same plasma treated sample results in marginal D and D' peaks, I_{2D}/I_G of 1.3 and no shift and broadening of the peaks compared to reference sample. This observation suggests that graphene is hydrogenated during H_2 plasma treatment largely contributing to the intense D peak and to graphene doping. The hydrogenation is found to be reversible through vacuum annealing. The weak D' peak and reduced I_{2D}/I_G could be due to induced strain in the graphene lattice [74, 75]. Therefore, we can conclude that H_2 high density ICP plasma is harmless for graphene even at high power and in non-downstream mode.

4. Conclusion

We show that high density H_2 and He plasma operated in a “clean” plasma chamber damage the materials constituting the plasma chamber, releasing oxygen atoms, halogens and metallic impurities in the plasma. Subsequently, these atoms damage the graphene irreversibly. We find that the only solution to get rid of such parasitic species in H_2 plasmas is to use a wafer holder made of Aluminum oxide and to fully fluorinate the chamber walls and the wafer holder with a F-rich plasma prior to the plasma treatment of graphene. In this case, F atoms are the only impurity in the H_2 plasmas. F atoms, when not ionized, are harmless to graphene because they cannot stick on it as evidenced in this study. However, if the plasma conditions damage graphene (by sputtering or chemical etching), F atoms impurities present in the reactor immediately stick to dangling bonds on graphene defects. The amount of F is actually a good indication of the amount of damages. Under well controlled conditions, we find that the H_2 high density ICP plasma can clean PMMA residues from graphene irrespective to its underlying substrate and without damaging irreversibly the graphene lattice. In addition, a two-step process is required to prevent the lift-off of the graphene layer caused by H intercalation between graphene and SiO_2 layer: PMMA residues should be cleaned before lift-off. The electrical property measurement of the cleaned graphene which is currently in progress, will further demonstrate the integrity of the cleaned graphene film as well as the harmless nature of the H_2 plasma cleaning process. Nevertheless, this dry-cleaning has the advantage to be an industrially mature technology adapted to large area substrates as well as to other 2D materials and heterostructures. In contrast, we find that graphene is systematically damaged when exposed to He plasmas and the extent of the

damages are mostly controlled by the plasma conditions. This difference is attributed to the high ionization energy threshold of He compared to H₂: in He, the impurities (including F) are ionized and bombard the graphene with an energy that is too high to prevent damages.

Supplementary Material

See the supplementary material for the additional XPS and Raman data.

Acknowledgements

The authors acknowledge the financial support from the French Agence Nationale de la Recherche in the frame of the project cleanGRAPH (ANR-13-BS09-0019) and from the French Government program “Investissements d’Avenir” managed by the National Research Agency (ANR) under the Contract No. ANR-10-IQPX-33. This work was also partly supported by the French RENATECH network.

References

- [1] Peltekis N et al 2012 The effect of downstream plasma treatments on graphene surfaces *Carbon* 50 395–403.
- [2] Cunge G et al 2015 Dry efficient cleaning of poly-methyl-methacrylate residues from graphene with high density H₂ and H₂-N₂ plasmas *J. Appl. Phys.* 118 123302.
- [3] Yang S-K et al. 2013 H₂ plasma characteristics for photoresist stripping *J. Semicond. Technol. Sci.* 13 387-394.
- [4] Lim Y-D et al 2012 Si-compatible cleaning process for graphene using low-density inductively coupled plasma *ACS Nano* 6 4410–4417.
- [5] Hazra K S et al 2011 Thinning of multilayer graphene to monolayer graphene in a plasma environment *Nanotechnology* 22 025704.
- [6] Prado M C et al 2013 Optimization of graphene dry etching conditions via combined microscopic and spectroscopic analysis *Appl. Phys. Lett.* 102 193111.
- [7] Shi Z et al 2011 Patterning graphene with zigzag edges by self-aligned anisotropic etching *Adv. Mater.* 23 3061–3065.
- [8] Lim W S et al 2012 Atomic layer etching of graphene for full graphene device fabrication *Carbon* 50 429-435.
- [9] Kim K S et al 2017 Atomic layer etching of graphene through controlled ion beam for graphene-based electronics *Scientific Reports* 7 2462.
- [10] Kim J H et al 2015 Large-scale plasma patterning of transparent graphene electrode on flexible substrates *Langmuir* 31 2914-2921.
- [11] Jeong S-J et al 2016 Self-aligned multichannel graphene nanoribbon transistor arrays fabricated at wafer scale *Nano Lett.* 16 5378-5385.
- [12] Bai J et al 2009 Rational fabrication of graphene nanoribbons using a nanowire etch mask *Nano Lett.* 9 2083-2087.

[13] Sun J et al 2015 Lateral plasma etching enhanced on/off ratio in graphene nanoribbon field-effect transistor Appl. Phys. Lett. 106 033509.

[14] Seo D H et al 2011 Thinning vertical graphenes, tuning electrical response: from semiconducting to metallic J. Mater. Chem. 21 16339

[15] Xie L 2010 et al Selective etching of graphene edges by hydrogen plasma. J. Am. Chem. Soc. 132 14751– 14753.

[16] Ryu G H et al 2017 Effects of dry oxidation treatments on monolayer graphene 2D Mater. 4 024011.

[17] Kim D C et al 2009 The structural and electrical evolution of graphene by oxygen plasma-induced disorder Nanotechnology 20 375703.

[18] Eren B et al 2012 Pure hydrogen low-temperature plasma exposure of HOPG and graphene: Graphane formation? Beilstein J. Nanotechnol. 3 852-859.

[19] Choi M S et al 2011 Plasma treatments to improve metal contacts in graphene field effect transistor J. Appl. Phys. 110 073305.

[20] Gokus T et al 2009 Making graphene luminescent by oxygen plasma treatment ACS Nano 3 3963–3968.

[21] Eren B et al 2015 Spectroscopic ellipsometry on Si/SiO₂/graphene tri-layer system exposed to downstream hydrogen plasma: Effects of hydrogenation and chemical sputtering Appl. Phys. Lett. 106 011904.

[22] Luo Z Q et al 2009 Thickness-dependent reversible hydrogenation of graphene layers ACS Nano 3 1781–1788.

[23] Russo J et al 2014 Controlling protein adsorption on graphene for cry-EM using low energy H₂ plasma Nat. Methods 11 649.

[24] Zhang X et al 2015 X-ray spectroscopic investigation of chlorinated graphene: Surface structure and electronic effects Adv. Funct. Mater. 25 4163-4169.

[25] Ferrah D et al 2016 XPS investigations of graphene surface cleaning using H₂- and Cl₂-based inductively coupled plasma Surf. Interface Anal. 48 451-455.

[26] Wu J et al 2011 Controlled chlorine plasma reaction for noninvasive graphene doping J. Am. Chem. Soc. 133 19668-19671.

[27] Walton S G et al 2017 Electron beam generated plasmas for the processing of graphene J. Appl. Phys. D: Appl. Phys. 50 354001.

[28] Al-Harhi S H et al 2012 Evolution of surface morphology and electronic structure of few layer graphene after low energy Ar⁺ ion irradiation Appl. Phys. Lett. 101 213107.

[29] Hug D et al 2017 Anisotropic etching of graphite and graphene in a remote hydrogen plasma npj 2D Materials and Applications 1 21.

[30] Eren B et al 2013 Hydrogen plasma microlithography of graphene supported on a Si/SiO₂ substrate Appl. Phys. Lett. 102 071602.

[31] Yang R et al 2010 An anisotropic etching effect in the graphene basal plane Adv. Mater. 22 4014.

[32] Elias D C et al 2009 Control of graphene's properties by reversible hydrogenation: Evidence for graphane Science 323 610–613.

- [33] Craciun M et al 2013 Properties and applications of chemically functionalized graphene J. Phys.: Condens. Matter. 25 423201.
- [34] Felten A et al 2014 Insight into hydrogenation of graphene: Effect of hydrogen plasma chemistry Appl. Phys. Lett. 105 183104.
- [35] Felten A et al 2013 Controlled modification of mono- and bilayer graphene in O₂, H₂ and CF₄ plasmas Nanotechnology 24 355705.
- [36] Diankov G et al 2013 Extreme monolayer-selectivity of hydrogen-plasma reactions with graphene ACS Nano 7 1324-1332.
- [37] Gouil A Le et al 2006 Chemical analysis of deposits formed on the reactor walls during silicon and metal gate etching processes J. Vac. Sci. Technol. B 24 2191.
- [38] Ullal S J et al 2002 Maintaining reproducible plasma reactor wall conditions: SF₆ plasma cleaning of films deposited on chamber walls during Cl₂/O₂ plasma etching of Si J. Vac. Sci. Technol. A 20 1195.
- [39] Cunge G et al 2012 Measurement of free radical kinetics in pulsed plasmas by UV and VUV absorption spectroscopy and by modulated beam mass spectrometry Plasma Sources Sci. Technol. 21 024006.
- [40] Banna S et al 2009 Inductively coupled pulsed plasmas in the presence of synchronous pulsed substrate bias for robust, reliable, and fine conductor etching IEEE Trans. Plasma Sci. 37 1730–1746.
- [41] Petit-Etienne C et al 2011 Etching mechanisms of thin SiO₂ exposed to Cl₂ plasma J. Vac. Sci. Technol. B 29 51202.
- [42] Ramos R et al 2007 Cleaning aluminum fluoride coatings from plasma reactor walls in SiCl₄/Cl₂ plasmas Plasma Sources Sci. Technol. 16 711.
- [43] Banna S et al 2009 Inductively coupled pulsed plasmas in the presence of synchronous pulsed substrate bias for robust, reliable, and fine conductor etching IEEE Trans. Plasma Sci. 37 1730–1746.
- [44] Braithwaite N S J et al 1996 A novel electrostatic probe for ion fluxes measurements Plasma Sources Sci. Technol. 5 677.
- [45] Darnon M et al 2014 Time-resolved ion flux, electron temperature and plasma density measurements in a pulsed Ar plasma using a capacitively coupled planar probe Plasma Sources Sci. Technol. 23 025002.
- [46] Brihoum M et al 2013 Ion flux and ion distribution function measurements in synchronously pulsed inductively coupled plasmas J. Vac. Sci. Technol. A 31 020604.
- [47] Banna S et al 2012 Pulsed high-density plasmas for advanced dry etching processes J. Vac. Sci. Technol. A 30 040801.
- [48] Ullal S J et al 2002 Maintaining reproducible plasma reactor wall conditions: SF₆ plasma cleaning of films deposited on chamber walls during Cl₂/O₂ plasma etching of Si J. Vac. Sci. Technol. A 20 1195.
- [49] Despiiau-pujo E et al 2016 Hydrogen Plasmas Processing of Graphene Surfaces Plasma Chem. Plasma Processing 36 213-229.

- [50] Duong D L et al 2012 Probing graphene grain boundaries with optical microscopy *Nature* **490** 235-239.
- [51] Nourbakhsh A et al 2010 Bandgap opening in oxygen plasma-treated graphene *Nanotechnology* **21** 435203.
- [52] Cunge G *et al* 2005 New chamber walls conditioning and cleaning strategies to improve the stability of plasma processes *Plasma Sources Sci. Technol.* **14** 599-609.
- [53] Georgakilas V et al 2012 Functionalization of Graphene: Covalent and Non-Covalent Approaches, Derivatives and Applications *Chem. Rev.* **112** 6156-6214.
- [54] Ao Z et al 2015 Enhancement of the stability of fluorine atoms on defective graphene and at graphene/fluorographene interface *ACS Appl. Mater. Interfaces* **7** 19659-19665.
- [55] Jansen H et al 1996 A survey on the reactive ion etching of silicon in microtechnology *J. Micromech. Microeng.* **6** 14-28.
- [56] Yang D et al 2009 Chemical analysis of graphene oxide films after heat and chemical treatments by X-ray photoelectron and Micro-Raman spectroscopy *Carbon* **47** 145–152.
- [57] Jinglei P et al 2014 Carbon impurities on graphene synthesized by chemical vapor deposition on platinum *J. Appl. Phys.* **116** 044303.
- [58] Barinov A et al 2009 Imaging and spectroscopy of multiwalled carbon nanotubes during oxidation: defects and oxygen bonding *Adv. Mater.* **21** 1916.
- [59] Artyushkova K et al 2001 Quantification of PVC-PMMA polymer blend compositions by XPS in the presence of x-ray degradation effects *Surf. Interface Anal.* **31** 352.
- [60] Gomez-Navarro C et al 2010 Atomic structure of reduced graphene oxide *Nano Lett.* **10** 1144–1148.
- [61] Chuvilin A et al 2009 From graphene constrictions to single carbon chains *New J. Phys.* **11** 083109.
- [62] Despiau-pujo E et al 2013 Elementary processes of H₂ plasma-graphene interaction: A combined molecular dynamics and density functional theory study *J. Appl. Phys.* **113** 114302.
- [63] Delfour L et al 2016 Cleaning graphene: A first quantum/classical molecular dynamics approach *J. Appl. Phys.* **119** 125309.
- [64] Katin K P et al 2017 Chemisorption of hydrogen atoms and hydroxyl groups on stretched graphene: A coupled QM/QM study *Phys. Lett. A* **381** 2686-2690.
- [65] Mendez I et al 2010 On the ionic chemistry in DC cold plasmas of H₂ with Ar *Phys. Chem. Chem. Phys.* **12** 4239-4245.
- [66] Cunge G et al 2002 Ion flux composition in HBr/Cl₂/O₂ and HBr/Cl₂/O₂/CF₄ chemistries during silicon etching in industrial high-density plasmas *J. Vac. Sci. Technol. B* **20** 2137-2148.
- [67] Haynes W M 2009 CRC handbook of chemistry and physics: A ready-reference book of chemical and physical data (Boca Raton: CRC Press).
- [68] Lin Y C 2012 et al Graphene annealing: How clean can it be? *Nano Lett.* **12** 414–419.
- [69] Nemes-Incze P et al 2010 Crystallographically selective nanopatterning of graphene on SiO₂ *Nano Res.* **3** 110–116.
- [70] Davydova A et al 2015 Etching mechanisms of graphene nanoribbons in downstream H₂ plasmas: insights from molecular dynamics simulations *J. Phys. D: Appl. Phys.* **48** 195202.

[71] Despiau-pujo E et al 2017 H⁺ ion-induced damage and etching of multilayer graphene in H₂ plasmas J. Appl. Phys. 121 133301.

[72] Ferrari A C et al 2004 Raman spectroscopy of amorphous, nanostructured, diamond-like carbon, and nanodiamond Philos. Trans. R. Soc. London A 362 2477–2512.

[73] Ferrari A C et al 2006 Raman spectrum of graphene and graphene layers Phys. Rev. Lett. 97 187401.

[74] Y.Y. Wang Y Y et al 2008 Raman studies of monolayer graphene: the substrate effect J. Phys. Chem. C 112 10637–10640.

[75] Ferrari A C 2007 Raman spectroscopy of graphene and graphite: disorder, electronphonon coupling, doping and nonadiabatic effects Solid State Commun. 143 47–57.

[76] Casiraghi C 2009 Doping dependence of the Raman peaks intensity of graphene close to the Dirac point Phys. Rev. B 80 233407.

[77] Das A et al 2008 Monitoring dopants by Raman scattering in an electrochemically top-gated graphene transistor Nature Nanotech. 3 210-215.

ACCEPTED MANUSCRIPT

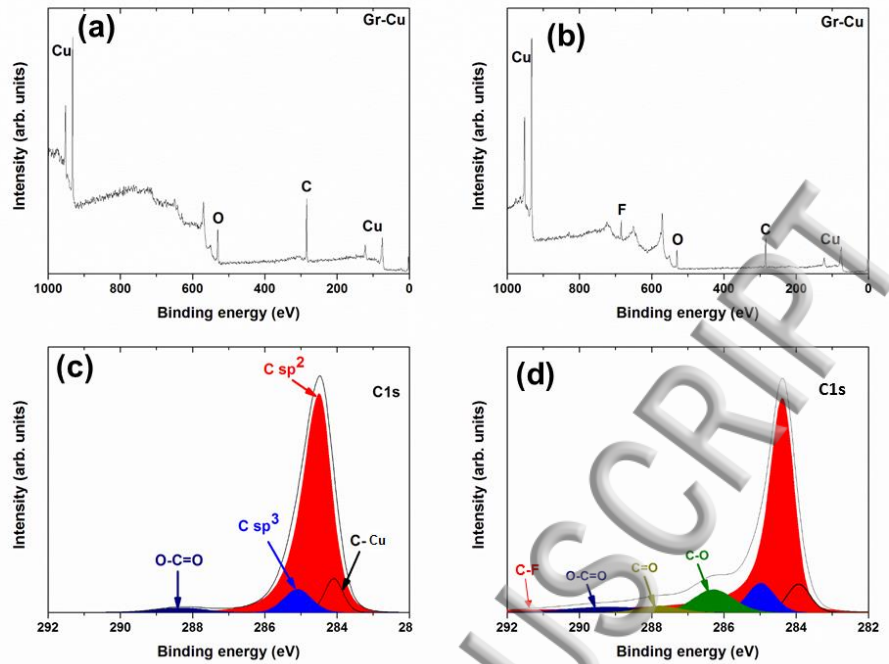


Figure 1. (a-b) Survey XPS spectra measured on CVD graphene/Cu: (a) reference before He plasma treatment and (b) after He plasma treatment in a clean reactor with chamber walls made of Al_2O_3 . (c-d) Corresponding C1s XPS spectra: (c) before and (d) after He plasma treatment revealing the presence of parasitic oxygen and fluorine atoms in the plasma. Prior to He plasma treatment, the ICP reactor is first cleaned with SF_6 plasma [48, 52]. Then, He plasma is run first without the graphene sample and then with the sample. The small graphene sample is fixed on a Si wafer of 300 mm diameter. The He plasma treatment conditions are as follows: 50 W ICP power, 300 mT chamber pressure, 30 sec treatment time and 200 sccm He flow.

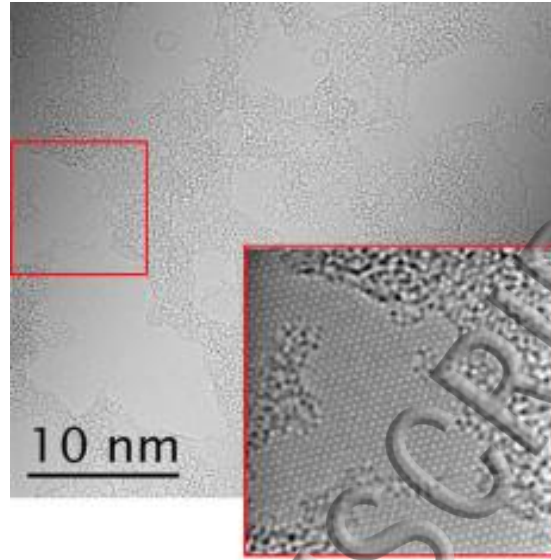


Figure 2. HRTEM image of CVD monolayer graphene transferred on Si_3N_4 TEM grid after H_2 plasma treatment. The red square and the associated inset indicate a region where several layer-thick PMMA is observed. These regions are systematically associated with the presence of heavier silicon impurity atoms (that appears darker) especially on the edges of the flakes of residues. Prior to H_2 plasma treatment, the ICP reactor is first cleaned with SF_6 plasma [48, 52]. Then, H_2 plasma is run first without the graphene sample and then with the sample. The small graphene sample is fixed on a Si wafer of 300 mm diameter. The H_2 plasma treatment conditions are as follows: 800 W ICP power, 200 mT chamber pressure, 30 sec treatment time and 200 sccm H_2 flow.

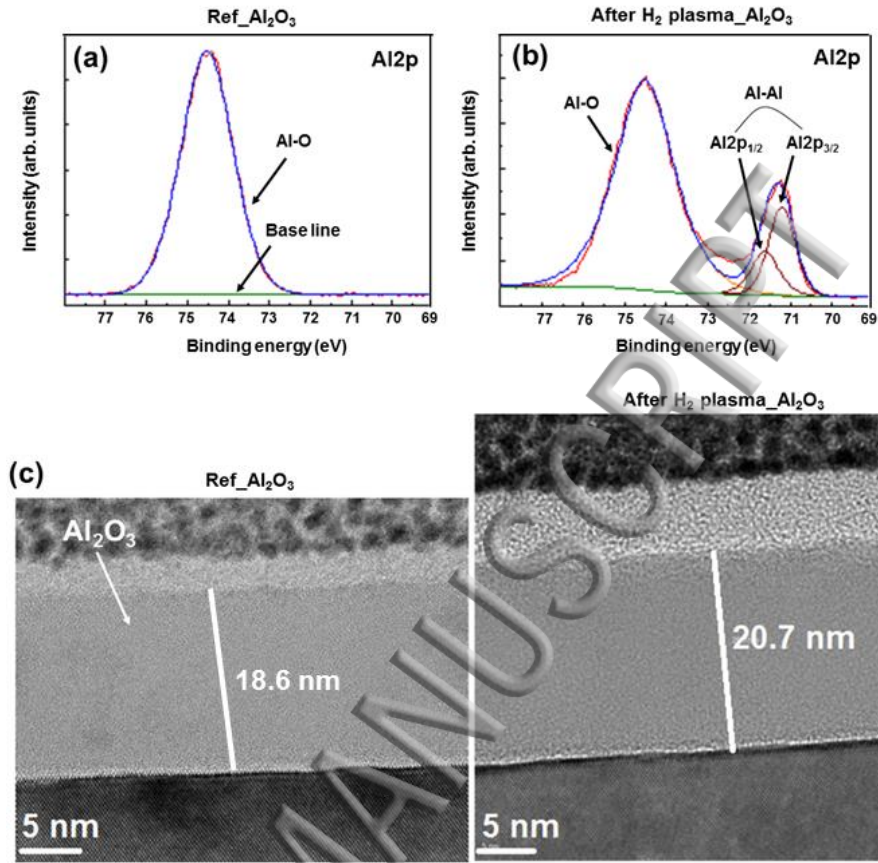


Figure 3. (a-b) XPS Al₂p spectra measured on the 300 mm diameter Al₂O₃ wafer (a) before and (b) after H₂ plasma treatment in a clean ICP reactor with Al₂O₃ chamber wall. (c) Cross-sectional HRTEM image of the same sample before and after the plasma treatment. Prior to H₂ plasma treatment, the ICP reactor is first cleaned with SF₆ plasma [48, 52]. Then, H₂ plasma is run first without the sample and then with the sample. The H₂ plasma treatment conditions are as follows: 800 W ICP power, 200 mT chamber pressure, 20 min treatment time and 200 sccm H₂ flow.

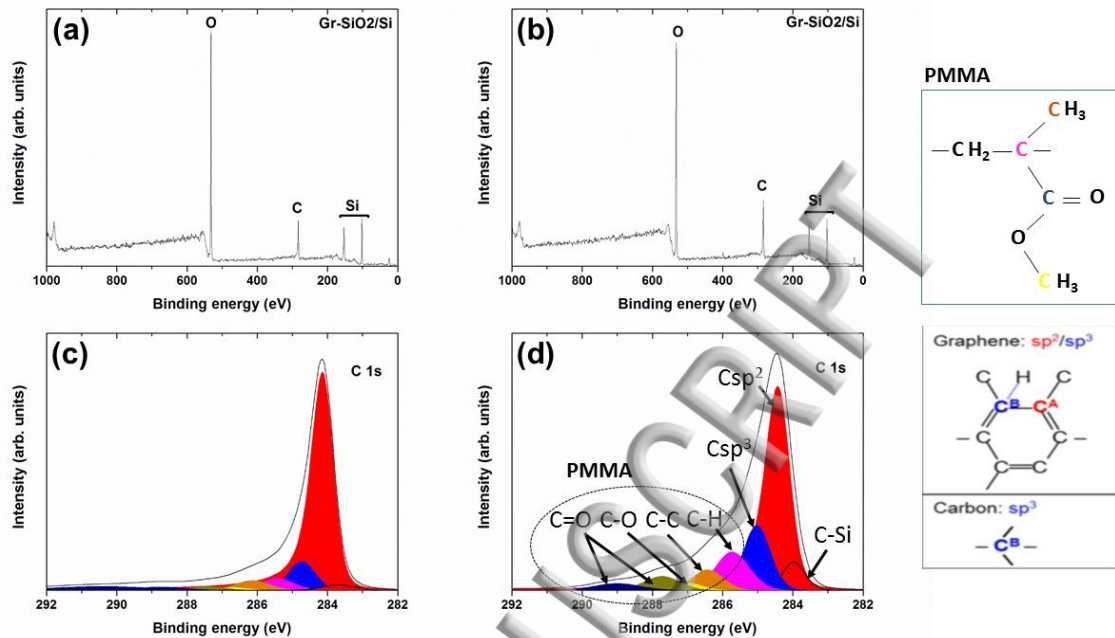


Figure 4. (a-b) Survey XPS spectra measured on graphene/SiO₂/Si: (a) reference before plasma and (b) after 30 sec H₂ plasma treatment. (c-d) corresponding C1s XPS spectra: (c) before and (d) after the plasma treatment. The increase in the carbon peak intensity in (b) indicates the contamination of the graphene surface with carbon released from the reactor wall during the plasma treatment, as is also confirmed by the increase in the carbon containing components in graphene as well as in PMMA (d). The inset on the upper right hand side is a schematic representation of the various carbon components present in PMMA and graphene. Prior to H₂ plasma treatment, the 300 mm diameter Al₂O₃ carrier wafer was treated with SF₆/O₂ plasmas, and the ICP reactor was treated with CH₄ plasmas. Therefore, the surface of the Al₂O₃ carrier wafer is fluorinated while the chamber walls are coated by a thick layer of carbon. Then, the H₂ plasma treatment was carried out with the following conditions: 800 W ICP power, 200 mT chamber pressure, 30 sec and 200 sccm H₂.

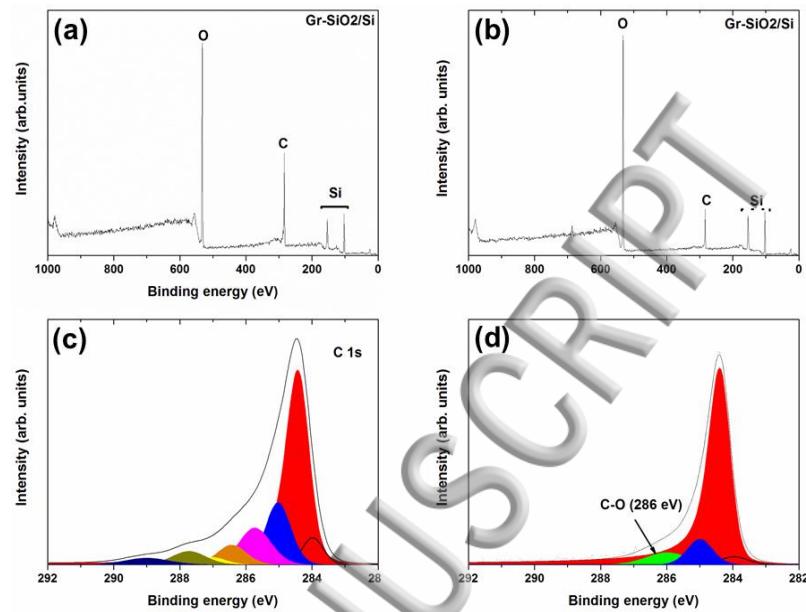


Figure 5. (a-b) survey XPS spectra measured on graphene/SiO₂/Si; (a) reference before plasma and (b) after H₂ plasma treatment. (c-d) corresponding C1s XPS spectra; (c) before and (d) after H₂ plasma treatment indicating removal of various carbon components in PMMA as well as removal of carbon residues in graphene as confirmed by the decrease in Csp³ peak intensity (blue curve in (d)). The appearance of the C-O peak, as indicated by arrow in (d), suggests graphene contamination with oxygen. Prior to H₂ plasma treatment, both the carrier wafer and the ICP reactor were treated with SF₆/O₂ plasmas. Under these conditions, both the chamber walls and the wafer holder are fluorinated alumina. Then, the plasma treatment was carried out in 2 steps: step-1) 800 W ICP power, 200 mT chamber pressure, 30 sec, 200 sccm H₂, step-2) 800 W ICP power, 80 mT, 60 sec, 200 sccm H₂.

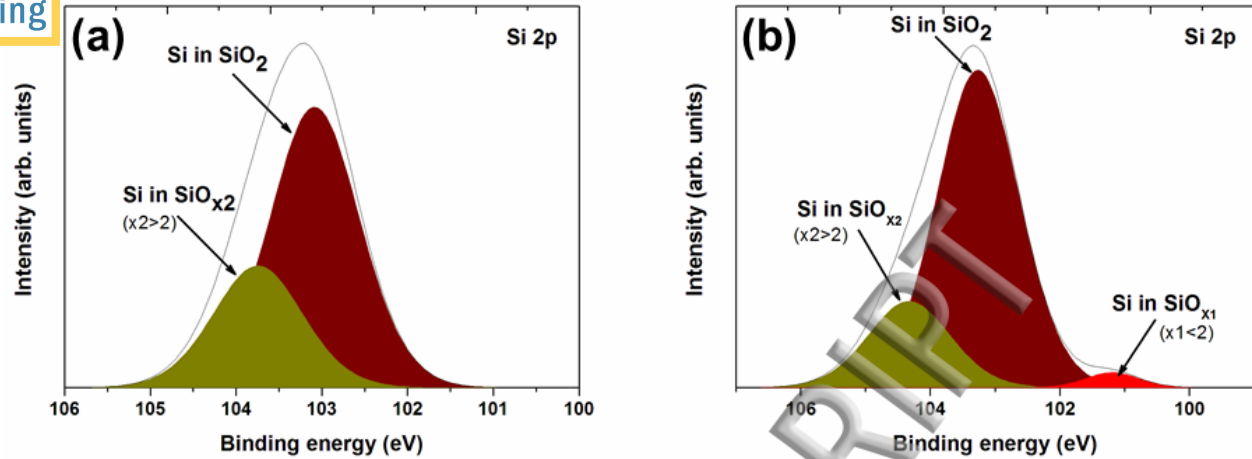


Figure 6. Si2p XPS spectra of graphene/SiO₂/Si; (a) reference before H₂ plasma treatment and (b) after H₂ plasma treatment in the fluorine-coated ICP reactor with fluorine coated 300 mm carrier wafer (20 nm Al₂O₃ on 500 μm Si). The appearance of the SiO_{x1} peak in the lower binding energy (d) demonstrates a partial reduction of the 300 nm SiO₂ layer underneath graphene during H₂ plasma exposure. The plasma treatment was carried out in 2 steps: step-1) 800 W ICP power, 200 mT chamber pressure, 30 sec, 200 sccm H₂, step-2) 800 W ICP power, 80 mT, 60 sec, 200 sccm H₂.

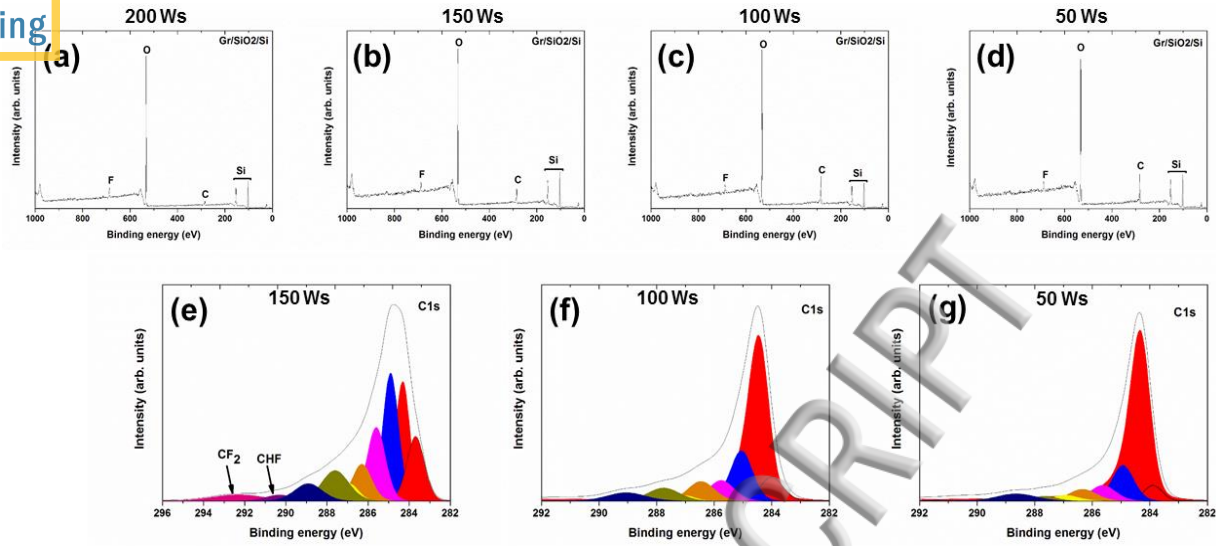


Figure 7. (a-d) Survey XPS and (e-g) corresponding C1s spectra measured on He plasma treated graphene/Cu at different ICP powers with fixed chamber pressure (300 mT) treatment time (30 sec) and He flow rate (200 sccm). The plasma treatment is carried out in the fluorine-coated ICP reactor with graphene/Cu fixed on the fluorine coated 300 mm Al₂O₃ carrier wafer.

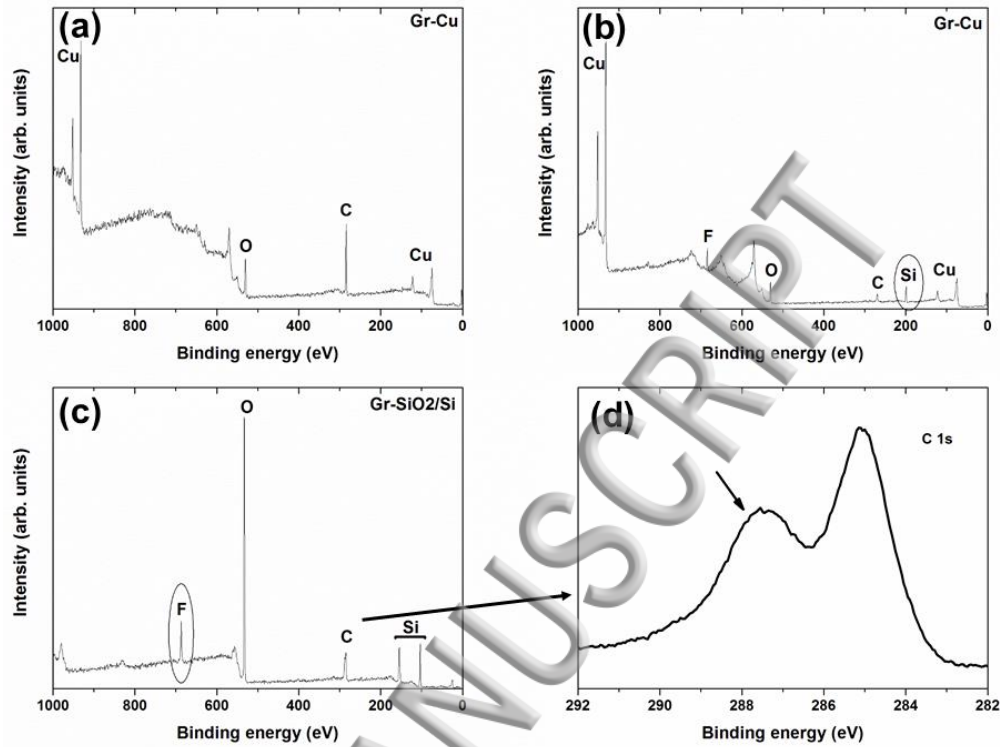


Figure 8. Survey XPS spectra measured on H₂ plasma treated graphene/Cu and graphene/SiO₂/Si with different carrier wafers. (a) reference graphene/Cu before H₂ plasma treatment and (b) after H₂ plasma treatment in the fluorine coated ICP reactor with 300 mm Si carrier wafer indicating graphene etching as well as contamination with Si. (c) graphene/SiO₂/Si after H₂ plasma treatment in the fluorine coated ICP reactor with fluorine coated 300 mm aluminum (Al) carrier wafer indicating graphene contamination with fluorine and (d) corresponding C 1s spectrum shows appearance of C-F component confirming fluorine contamination. The plasma treatment was carried out with the following conditions: 800 W ICP power, 200 mT chamber pressure, 30 sec and 200 sccm H₂.

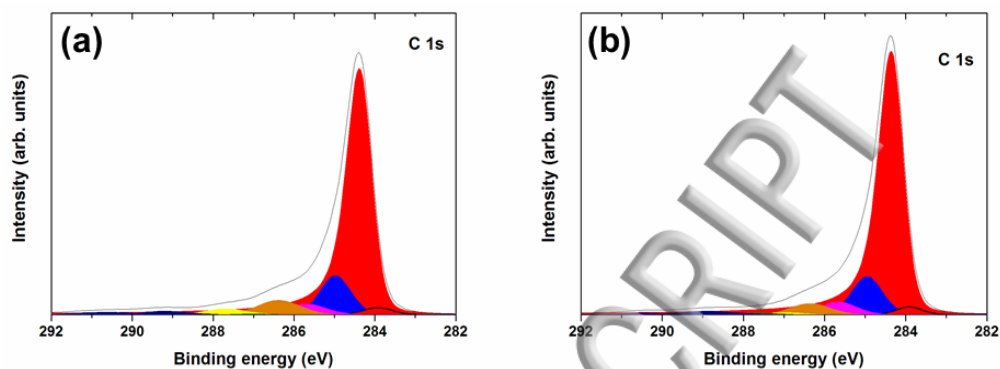


Figure 9. C1s XPS spectra measured on graphene/SiO₂/Si after treated with (a) H₂ plasma conditions of the step-1: 800 W ICP power, 200 mT chamber pressure, 30 sec, 200 sccm H₂ and (b) H₂ plasma conditions of the step-2: 800 W ICP power, 80 mT, 60 sec, 200 sccm H₂ indicating the presence of PMMA residues on the graphene surface after H₂ plasma treatment.

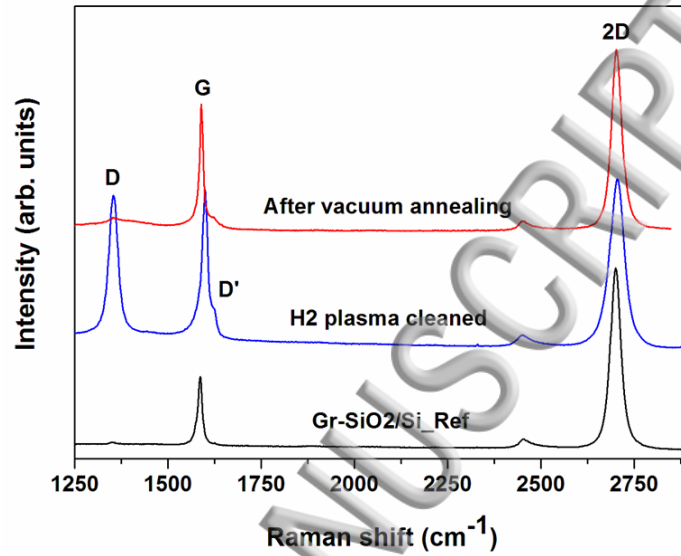


Figure 10. Raman spectra of graphene/SiO₂/Si (a) reference before H₂ plasma treatment, (b) after H₂ plasma treatment and (c) after vacuum annealing at 450 °C for 60 min. Laser wavelength was 488 nm. Prior to H₂ plasma, both the ICP reactor walls and the carrier wafer surface (20 nm Al₂O₃ on Si) were fluorine coated. The plasma treatment was carried out in 2 steps: step-1) 800 W ICP power, 200 mT chamber pressure, 60 sec, 200 sccm H₂, step-2) 800 W ICP power, 80 mT, 30 sec, 200 sccm H₂.